



Contents lists available at ScienceDirect

# Spectrochimica Acta Part A: Molecular and Biomolecular Spectroscopy

journal homepage: [www.elsevier.com/locate/saa](http://www.elsevier.com/locate/saa)

## Fabrication of 2D nanosheet through self assembly behavior of sulfamethoxypyridazine inclusion complexes with $\alpha$ - and $\beta$ -cyclodextrins



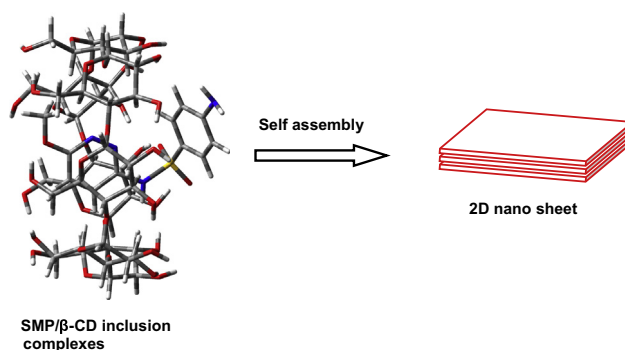
N. Rajendiran\*, G. Venkatesh, T. Mohandass

Department of Chemistry, Annamalai University, Annamalainagar 608 002, Tamilnadu, India

### HIGHLIGHTS

- 2D nanosheet structures are formed in sulfamethoxypyridazine/ $\beta$ -CD inclusion complex.
- Self assembled nanorods are formed in sulfamethoxypyridazine/ $\alpha$ -CD inclusion complex.
- Intermolecular hydrogen bonding play a vital role in the supramolecular self assembling process.
- The size of the CD determined the shape of the supramolecular architecture.

### GRAPHICAL ABSTRACT



### ARTICLE INFO

#### Article history:

Received 22 October 2013

Received in revised form 26 November 2013

Accepted 4 December 2013

Available online 18 December 2013

#### Keywords:

Sulfamethoxypyridazine

Cyclodextrins

Molecular modeling

2D nanosheet

Supramolecular architecture

Pseudopolyrotaxane

### ABSTRACT

A 2D nanosheet was fabricated through the supramolecular self assembly of sulfamethoxypyridazine (SMP) and  $\beta$ -cyclodextrin ( $\beta$ -CD) inclusion complexes. HRTEM image exhibited 2D nanosheet morphology with a length of 1200 nm and the sheet thickness of 60 nm. It is noted that the nanosheet did not form a single layer aggregation but a bulk aggregation of SMP/ $\beta$ -CD inclusion complex. The formation of this multilayer 2D nanosheet based on the self assembly of SMP/ $\beta$ -CD inclusion complexes is proposed by the topological transformation as well as molecular modeling calculations. But, nanorods are formed in SMP/ $\alpha$ -CD inclusion complex indicated that the nature of the CD determined the shape of the self assembled supramolecular architecture. The formation of nanomaterial was characterized by using FT-IR, DSC, PXRD,  $^1\text{H}$  NMR, absorption, fluorescence and lifetime measurements.

© 2013 Elsevier B.V. All rights reserved.

### Introduction

In the past decade, considerable interest has been shown in the development of new vectors based on different hydrophobic CD derivatives. These macrocyclic amphiphiles can form a variety of supramolecular assemblies, such as micelles [1,2], vesicles [3,4], and nanoparticles [5–7]. In this area, amphiphilic  $\alpha$ -cyclodextrins

obtained by grafting aliphatic chains on the primary or secondary face exhibit self-organizational properties yielding stable nanospheres or nanocapsules [8–10]. A good knowledge of the nanoaggregate ultra structure is essential to the development of drug carriers. It is worth reminding that the ability to encapsulate drugs is partly related to the internal structure of nanosystems.

The studies of inclusion complexes are important in fundamental research since it furnishes valuable information about noncovalent intermolecular forces [11]. Apart from this, research in the field of characterization of inclusion complexes has experienced a

\* Corresponding author. Tel.: +91 94866 28800; fax: +91 41442 38080.

E-mail address: [drrajendiran@rediffmail.com](mailto:drrajendiran@rediffmail.com) (N. Rajendiran).

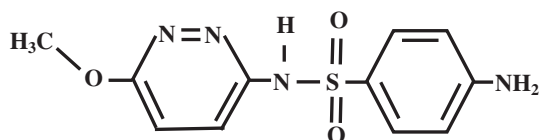


Fig. 1. Chemical structure of SMP.

splendid evolution because of its potential ability in a diverse range of applications. These inclusion complexes can serve as miniature models for studying the mode of action of enzymes [12] mimicking the reactions in biosystems [13] and so forth. These, have promising prospects in future applications like drug delivery [14], nanometer-sized electronic devices, and development of energy storage devices [15]. In this article, we report the fabrication of 2D nanosheet through self assembly of  $\beta$ -cyclodextrin with sulfamethoxyypyridazine (Fig. 1) drug. The self assembled morphology was observed using transmission electron microscope (TEM) and scanning electron microscope (SEM). We proposed a reasonable formation mechanism for the formation of the 2D nanosheet. The inclusion complexes were subsequently characterized by FT-IR, differential scanning calorimeter (DSC), powder X-ray diffraction (PXRD),  $^1\text{H}$  NMR, absorption and fluorescence emission spectroscopy techniques. The sulfamethoxyypyridazine (SMP) belongs to a class of sulfonamide drugs, which is frequently used in pharmaceutical preparation, especially in veterinary practices. Interest in the field of drug studies are not only for gaining some fundamental insight into the determination of pharmaceutical samples, but also obtaining information about the structure as well as the cheating behavior of the drugs.

The aim of the present work was to study the self assembly behavior of SMP drug (Fig. 1) with  $\alpha$ -CD and  $\beta$ -CD. The absorption and fluorescence characteristics of few sulfa drugs with different solvents, pH and  $\beta$ -CD were already reported [16,17]. In our previous study we investigated inclusion complexation of some sulfonamide derivatives with  $\beta$ -CD. In the present work, we prepared solid inclusion complexes of the SMP drug with  $\alpha$ -CD and  $\beta$ -CD and the inclusion complexation behavior was characterized by UV-visible, fluorescence, life time, FTIR, DSC, PXRD,  $^1\text{H}$  NMR, SEM and TEM and techniques.

## Experimental section

### Materials

SMP,  $\alpha$ -CD and  $\beta$ -CD was purchased from Sigma-Aldrich chemical company and used without further purification. The purity of the compound was checked for similar fluorescence spectra when excited with different wavelengths.

### Preparation of nanomaterials

CD (1 mmol) was dissolved in 30 ml distilled water and SMP (1 mmol) in 20 ml methanol and was slowly added to the CD solution. This solution was stirred at 50 °C overnight. The above solution was refrigerated overnight at 5 °C. The precipitated SMP/CD complexes were recovered by filtration and washed with a small amount of ethanol and water to remove uncomplexed drug and CD, respectively. This precipitate was dried in vacuum at room temperature for two days and stored in an airtight bottle. This powder sample was used for further analysis.

### Preparation of CD solution

The concentration of stock solution of the drug was  $2 \times 10^{-3}$  M. The stock solution (0.2 ml) was transferred into 10 ml volumetric

flasks. To this, varying concentration of CD solution ( $1.0 \times 10^{-3}$  to  $1.0 \times 10^{-2}$  M) was added. The mixed solution was diluted to 10 ml with triply distilled water and shaken thoroughly. The final concentration of SMP in all the flasks was  $4 \times 10^{-5}$  M. The experiments were carried out at room temperature at 300 K.

### Instruments

Scanning electron microscopy (SEM) photographs were collected on a JEOL JSM 5610LV instrument. Morphology of the SMP inclusion complexes was investigated by transmission electron microscopy (TEM) using a TECNAI G2 microscope with accelerating voltage 200 kV. Carbon coated copper TEM grid (200 mesh) was used for TEM analysis. FT-IR spectra of SMP,  $\alpha$ -CD,  $\beta$ -CD and the inclusion complexes were recorded 4000–400  $\text{cm}^{-1}$  on Nicolet Avatar 360 FT-IR spectrometer.  $^1\text{H}$  NMR spectra for SMP and its inclusion complexes were recorded on a Bruker AVANCE 400 MHz spectrometer using DMSO- $d_6$  as a solvent. The differential scanning calorimeter (DSC) was recorded using Mettler Toledo DSC1 fitted with STR<sup>®</sup> software (Mettler Toledo, Switzerland). The temperature scanning range was from 25 to 220 °C with a heating rate of 10 °C/min. Powder X-ray diffraction (PXRD) spectra were recorded with a BRUKER D8 advance diffractometer (Bruker AXS GmbH, Karlsruhe, Germany), The XRD patterns were measured in the  $2\theta$  angle range between 5° and 80° with a scan rate 5°/min. Absorption spectral measurements were carried out with a Shimadzu (model UV 1650 PC) UV-visible spectrophotometer and steady-state fluorescence measurements were made by using a Shimadzu spectrofluorimeter (model RF-5301). The fluorescence lifetime measurements were performed using a picosecond laser and single photon counting setup from Jobin-Vyon IBH.

### Molecular modeling studies

The theoretical calculations were performed with Gaussian 03W package. The initial geometry of the SMP,  $\alpha$ -CD and  $\beta$ -CD was constructed with the aid of Spartan 08 and then optimized by the semiempirical PM3 method at vacuum. The CD was fully optimized by PM3 without any symmetry constraint [18]. The glycosidic oxygen atoms of CD were placed onto the XY plane and their center was defined as the center of the coordinate system. The primary hydroxyl groups were placed pointing toward the positive Z axis. The inclusion complex was constructed from the PM3 optimized CD and guest molecules. The longest dimension of the guest molecule was initially placed onto the Z axis. The position of the guest was determined by the Z coordinate of one selected atom of the guest. The inclusion process was simulated by putting the guest on one end of the CD and then letting it pass through the CD cavities. Since the semiempirical PM3 method has been proved to be a powerful tool in the conformational study of CD inclusion complexes and has high computational efficiency [19], we selected semiempirical PM3 method to study the inclusion process of CDs with the SMP drug.

## Results and discussion

### Micromorphological observations

The surface morphology of powder samples of SMP,  $\alpha$ -CD,  $\beta$ -CD, SMP/ $\alpha$ -CD and SMP/ $\beta$ -CD complexes were assessed by SEM. As illustrated in Fig. 2 SMP existed in a microcrystalline structure, whereas SMP/ $\alpha$ -CD inclusion complex appeared in the form of irregular particles in which the original morphology of both the SMP and  $\alpha$ -CD components disappeared and tiny aggregates of amorphous pieces of irregular shape were present. The SMP/ $\beta$ -CD

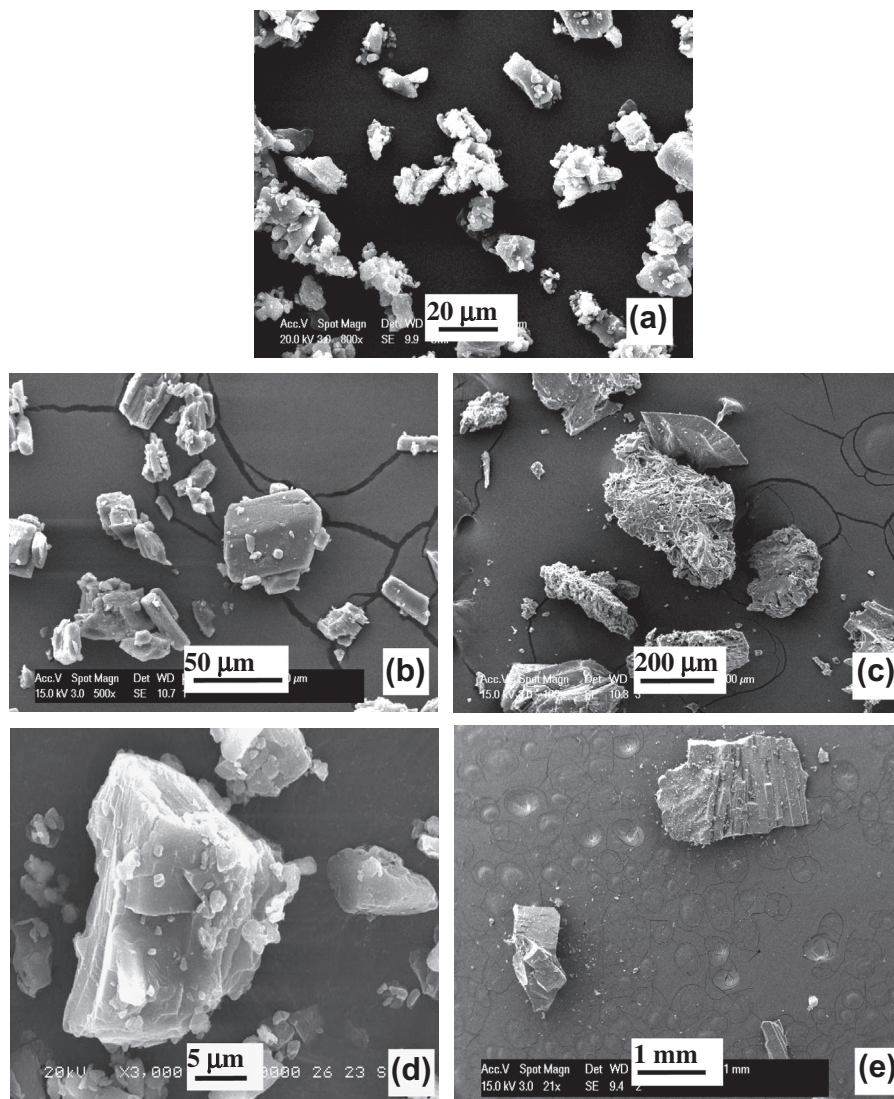


**Fig. 2.** SEM images of (a) SMP, (b)  $\alpha$ -CD, (c) SMP/ $\alpha$ -CD complex, (d)  $\beta$ -CD and (e) SMP/ $\beta$ -CD complex.

inclusion complex appeared as a micro-sheet like structure, which was formed by SMP and  $\beta$ -CD mixed with excipient particles or adhered to their surface. The comparison of these images revealed that the SMP/ $\alpha$ -CD and SMP/ $\beta$ -CD inclusion complexes were structurally distinct from the isolated components. The size and shape of the SMP/ $\alpha$ -CD inclusion complex were different from that SMP/ $\beta$ -CD inclusion complex, which confirmed the formation of different nanomaterials.

The HRTEM images in Fig. 3c shows the perfect architecture of the 2D nanosheet formed by the self aggregation of SMP/ $\beta$ -CD inclusion complexes, whereas the SMP/ $\alpha$ -CD shows a nanotube like structure (Fig. 3a and b). The SMP/ $\beta$ -CD inclusion complex act as a building blocks and has unique structural features for hierarchical supramolecular self assembly. The  $\alpha$ -CD and  $\beta$ -CD have two types of hydroxyl groups on the end of the cavities; one is a primary hydroxyl group (tail) and another is a secondary hydroxyl group (head). Probably, there are three types of arrangement modes in which CDs can have interacted with each others, namely head-to-head, tail-to-tail and head-to-tail. So, the intermolecular hydrogen bonding between the SMP/ $\beta$ -CD inclusion complexes play a vital role in the supramolecular self assembly. The primary and secondary hydroxyl groups of the CDs play an essential role in the formation of these types of 2D hybrid nanosheet through hydrogen bonding. According to the previous reports [20,21], the self-aggre-

gation proceeds mainly from the contribution of hydrogen bonding or electrostatic interactions. Further, the above reports indicate that the aggregation between CDs inclusion complexes is not only hydrogen bonding and nonbonding interactions like van der Waals forces, hydrophobic interaction, etc., and that they are also responsible for the formation of the well defined supramolecular architecture. Through these intermolecular forces, SMP/ $\beta$ -CD inclusion complexes are aggregated and form a 2D nanosheet like structure with the length of approximately 1200 nm.

Recently Chandrasekar and his co-workers [22] studied and demonstrated the reversible shape-shifting of organic nanostructures that have dimensionally dependent optical waveguides. And they were fabricated with organic rhombus shaped nanosheet by self assembling of novel triazole derivative in acetonitrile solutions. Besides, they reported that the triazole ring nitrogen atoms participate in the intermolecular hydrogen bonding, thus playing a crucial role in the supramolecular self assembling process. In the present case also the intermolecular hydrogen bonding interaction is the dominant driving force of the self assembling process.

#### *Formation mechanism of 2D nanosheet*

Based on our observations from the micromorphological images, we proposed the self assembling mechanism of 2D

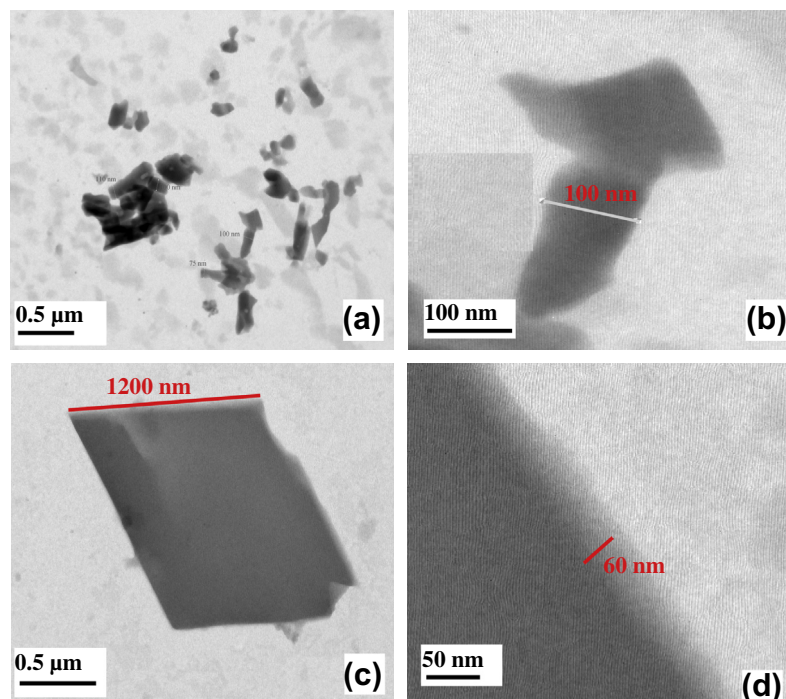


Fig. 3. TEM photographs of (a and b) SMP/ $\alpha$ -CD complex and (c and d) SMP/ $\beta$ -CD complex.

nanosheet formation. A closer examination of the nanosheet edges (Fig. 3d) showed that the thickness of the nanosheet is approximately 60 nm, which confirms that the nanosheet was not a single layer aggregation of SMP/ $\beta$ -CD inclusion complex, but it is a multi-layer bulk assembly of these complexes. The proposed mechanism is shown in Fig. 4. In the first stage, the individual SMP/ $\beta$ -CD complexes are arranged at one dimensionally ( $a$ -axis) to form a pseudopolyrotaxane like structure through intermolecular hydrogen bonding. These pseudopolyrotaxane further aggregates in the same molecular axis to form a single or a 1D molecular level layer (Fig. 4c). Again every primarily assembled single molecular level monolayer's are tightly stacked along another one molecular axis ( $b$ -axis). This process can go ahead to form 2D nanosheet like supramolecular self aggregates of SMP/ $\beta$ -CD inclusion complexes.

To find out the number of SMP/ $\beta$ -CD molecular level layers that make up the nanosheet, we performed molecular modeling studies we observed that on the single or individual SMP/ $\beta$ -CD inclusion complex. From the molecular modeling studies a single SMP/ $\beta$ -CD inclusion complex has an average height about 10.02 Å (1.002 nm). Hence, the 1D molecular level layer has a thickness of approximately 1.002 nm, because these individual inclusion complexes were arranged in one direction to form the 1D molecular level layer. Comparison of the molecular modeling studies and HRTEM data showed that the nanosheet approximately 60 nm thickness is composed of approximately 60 single molecular level layers ( $60 \times 1.002 \text{ nm} = 60.12 \text{ nm}$ ).

However, instead of  $\beta$ -CD, if  $\alpha$ -CD is used as the host molecule with SMP, the obtained SMP/ $\alpha$ -CD inclusion complexes have a nanorod like morphology, which is shown in Fig. 3a and b. The preparation method of SMP/ $\alpha$ -CD inclusion complex was same as that stated in the experimental part but the self assembling morphology of SMP/ $\alpha$ -CD and SMP/ $\beta$ -CD were different. This demonstrates that the self assembled 2D nanosheet architecture of the SMP/ $\beta$ -CD complex depending on the supramolecular assembly of  $\beta$ -CD with SMP drug, and the type of CD determines the shape of the self assembled architectures. The height of the nanorods varied from 225 nm to 640 nm and diameter of the nanorods varied from 75 nm to 200 nm. The short nanorod like structure of

SMP/ $\alpha$ -CD complex nanomaterial definitely stem from the replication of the cylindrical shape of pseudopolyrotaxane structure shown in Fig. 3b. So the same line of proposed mechanism has been taken in explaining the formation of nanorod structure of SMP/ $\alpha$ -CD complexes. Further, intermolecular forces as discussed earlier not much extended between the SMP/ $\alpha$ -CD that is why SMP/ $\alpha$ -CD complex having nanorod self assembly. The same type of results was reported by Chen and his co-workers [23], when they fabricated mesoporous silica microtubes through the self assembly behavior of  $\beta$ -CD and Triton X-100 micelles. Their reports indicate that  $\beta$ -CD acts as a structure directing agents to construct the mesoporous silica microtube.

#### FT-IR spectral analysis

FT-IR spectra in the region from 4000 to 400  $\text{cm}^{-1}$  of the uncomplexed SMP and the corresponding inclusion complexes are recorded (Fig. S1 in Supplementary material). It can be seen from the FT-IR spectra peak at 3466  $\text{cm}^{-1}$  in SMP molecule assign to the  $-\text{NH}_2$  stretching vibration, which can be moved to lower frequencies at 3402  $\text{cm}^{-1}$  for SMP/ $\alpha$ -CD complex and 3377  $\text{cm}^{-1}$  in SMP/ $\beta$ -CD complex. Such lower frequency shift for  $-\text{NH}_2$  stretching is due to the overlapping of this vibration into  $-\text{OH}$  stretching frequency of CDs. The frequency appeared at 2939  $\text{cm}^{-1}$  is assigned to the aromatic  $-\text{C}-\text{H}$  stretching vibration of free SMP molecules, and is moved to lower frequency of 2928  $\text{cm}^{-1}$  and 2926  $\text{cm}^{-1}$  for both  $\alpha$ -CD and  $\beta$ -CD inclusion complexes respectively. Another characteristic vibration in SMP molecule is  $-\text{S}=\text{O}$  stretching appeared at 1035  $\text{cm}^{-1}$  which strongly affected in both inclusion complexes ( $\sim 1028 \text{ cm}^{-1}$ ). The shift in the above frequency is due to the hydrogen bond formation between this sulfonyl group and CDs hydroxyl group. The stretching vibration at 2843  $\text{cm}^{-1}$  is due to the aliphatic  $-\text{CH}_3$  stretching of the SMP molecule and it completely vanished from the inclusion complexes. In the present study, there are difference between uncomplexed SMP and complexes with CDs in the relative intensity of the various peaks in spectrum region 1500–1200  $\text{cm}^{-1}$ . This probably provides evidence for the inclusion complex formation.

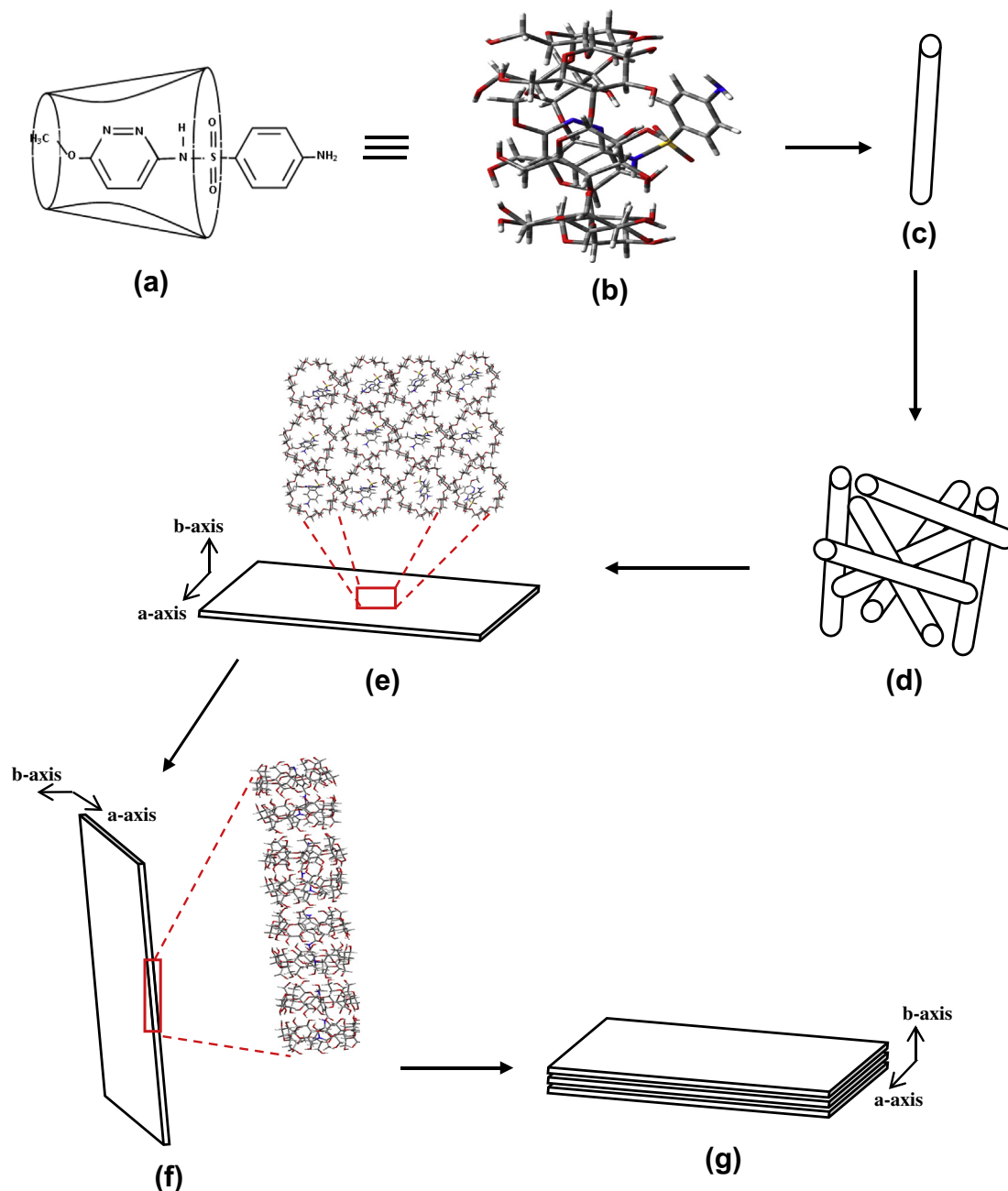


**Fig. 4.** Proposed mechanism for the formation of 2D nanosheet: (a and b) inclusion complexes of SMP/β-CD, (c and d) randomly oriented pseudopolyrotaxanes of SMP/β-CD inclusion complexes formed by hydrogen bonding, (e and f) a molecular layer level (1D nanosheet) aggregation of pseudopolyrotaxanes of SMP/β-CD inclusion complexes at molecular axis-a, (g) 1D molecular level layers are tightly stacked with another one molecular axis-b and form 2D nanosheet.

*DSC thermograms*

Encapsulation of SMP into both the CDs cavity has been confirmed by the DSC thermograms. Since the disappearance of thermal events of SMP molecule is considered as a proof of inclusion complex formation. Fig. S2 in Supplementary material shows the details about the DSC thermograms of α-CD, β-CD, SMP and its inclusion complexes. The DSC scans of SMP show an exothermic peak at 181.6 °C, which corresponds to melting point of the free SMP drug (Fig. S2c). The DSC curves of β-CD shows a broad endothermic peak around 128.6 °C and α-CD shows three endothermic peaks at 79.2 °C, 109.1 °C and 137.5 °C. These endothermic peaks are associated with crystal water loss from CDs. The thermogram of SMP/CD inclusion complexes prepared by co-precipitation method show the complete disappearance of the characteristic

endothermic peaks of both CDs and SMP drug thus implying complex formation. The SMP/α-CD complex show one endothermic peak at 96.4 °C and SMP/β-CD complex show two endothermic peaks at 84.6 °C and 128.6 °C. All the above endothermic peaks appear due to loss of water molecules from the CDs. The disappearance of the characteristic endothermic peak of SMP drug in the corresponding inclusion complexes thermogram is taken as an evidence for the formation of inclusion complexes.

*Powder X-ray diffraction analysis*

Powder X-ray diffraction patterns of SMP and their inclusion complexes are shown in Fig. S3 in Supplementary material. The diffraction peak of uncomplexed drug molecules and complexes with CDs are entirely different, suggesting that SMP drug forms

inclusion complexes with both CDs. Sharp peak observed in the diffractograms of the uncomplexed SMP confirmed the crystalline nature of the drugs. It is also revealed, from the diffractograms that the SMP enter into the CD cavity and modify the crystal lattice structure of the CD. Hence, the characteristic new peaks have appeared and become clearly distinct. A similar result was reported by Neoh and his co-workers [24] in complexation between CO<sub>2</sub> with  $\alpha$ -CD. The major diffraction peaks at an angle of  $2\theta = 8.7^\circ$ ,  $12.2^\circ$ ,  $13.4^\circ$ ,  $18.1^\circ$ ,  $22.6^\circ$ ,  $32.2^\circ$ ,  $35.4^\circ$  in the diffractogram of SMP (Fig. S3a) is significantly higher in intensity than that of the diffractograms of inclusion complexes with  $\alpha$ -CD (Fig. S3b) and  $\beta$ -CD (Fig. S3c). The present study implies that the significantly higher/lower intensities of the diffracted peaks are a result of the inclusion complex formation of these SMP drugs with both CDs. A new sharp peak appeared at angle  $18.6^\circ$  in the diffractogram of SMP/ $\alpha$ -CD, which was absent in the free SMP diffractograms indicating the formation of the inclusion complexes. The above result due to the inclusion of guest into the CDs cavity could cause the changes in the host and guest shape, which modified the diffraction patterns of the respective systems.

### <sup>1</sup>H NMR analysis

<sup>1</sup>H NMR is one of the most powerful tools for the identification of the formation of inclusion complexes and for the demonstration of total or partial inclusion in the CDs cavities that occurs in liquid medium. In the inclusion complexes, it is important to explain whether the guest molecule is fully or partially included in the CD cavity. During complex formation the chemical environment of the guest molecule changed, and this resulted in change in chemical shift of the <sup>1</sup>H NMR line of the guest protons that are due to the shielding or deshielding effects. The internal protons of the CD cavity (H-3 and H-5 protons) were responsible for the changes in the <sup>1</sup>H NMR peak position of the guest protons. <sup>1</sup>H NMR spectra of SMP and its complexes were recorded at 25 °C in DMSO-d<sub>6</sub>, the chemical shift values for the SMP and its inclusion complexes (in parentheses first value corresponds to  $\alpha$ -CD and the second corresponds to  $\beta$ -CD inclusion complex) are as follows, OCH<sub>3</sub> = 3.859 (3.813/3.886); NH<sub>2</sub> = 5.952 (5.313/5.251); Ar-H = 6.564 (6.659/6.631); Ar-H = 7.251 (7.237/7.241); Ar-H = 7.512 (7.548/7.569). The above results shows the chemical shift value of amino protons of SMP shift up to  $-0.639$  ppm (in  $\alpha$ -CD complex) and  $-0.701$  ppm (in  $\beta$ -CD complex) as compared with corresponding free SMP molecule. These results indicated that the amino part of the SMP molecule interacts strongly with CD cavities.

### Absorption and fluorescence spectral studies

Figs. 5 and S4 depicts the absorption and emission spectra of SMP ( $4 \times 10^{-5}$  M) in pH  $\sim 7$  solutions containing different concentrations of  $\alpha$ -CD and  $\beta$ -CD. The inset Figs 5 and S4 depicts the changes in the absorbance and fluorescence intensity was observed as a function of the concentration of CD added. In both CD solutions, the absorbance was not significantly increased. In  $\beta$ -CD solution a slight red shift was observed in SMP (320, 262, 230 nm to 323, 266, 232 nm), whereas no significant shift was observed in  $\alpha$ -CD solution. The above results indicate that both the drugs were transformed to more polar aqueous medium into less polar CDs cavities. The changes in the absorption band and molar extinction coefficient with the addition of both CDs suggest the formation of inclusion complexes between SMP with  $\alpha$ -CD and  $\beta$ -CD [25–30].

In aqueous medium SMP shows single emission maxima around  $\sim 330$  nm, this corresponds to the locally excited (LE) state. Upon addition of both  $\alpha$ -CD and  $\beta$ -CD to aqueous solutions of SMP they show a new structured longer wavelength (LW) emission around  $\sim 430$  nm. This LW emission is attributed to the formation of

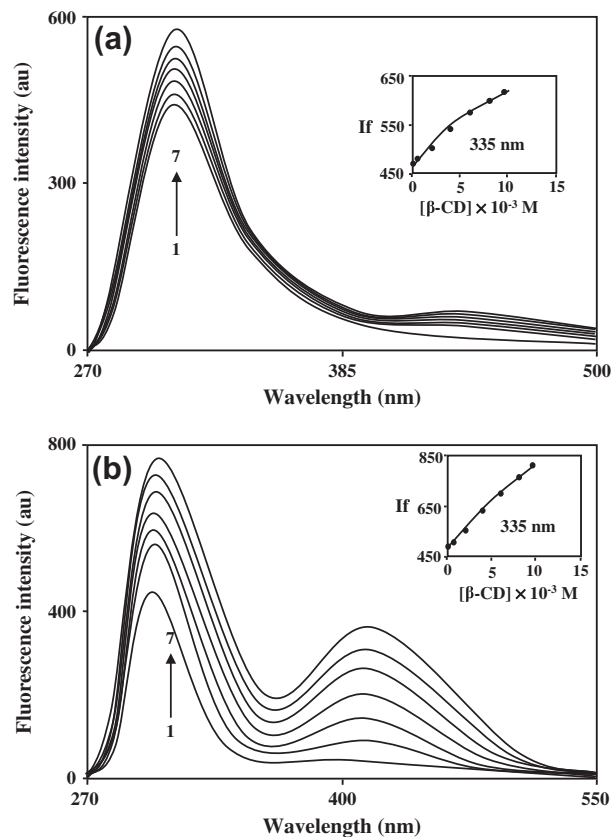


Fig. 5. Fluorescence spectra of SMP in different  $\alpha$ -CD and  $\beta$ -CD concentrations (M): (1) 0, (2) 0.001, (3) 0.002, (4) 0.004, (5) 0.006, (6) 0.008 and (7) 0.01 (Excitation wavelength: 260 nm).

inclusion complexes. The LW emission may correspond to an energy stabilization of emitting species and it is characteristic for the fluorescence of an intramolecular charge transfer (ICT) or twisted intramolecular charge transfer (TICT). The LW emission of SMP drugs originates from the TICT state and twisting occur S–N bond between aniline moiety (electron donor) and SO<sub>2</sub> moiety (electron acceptor). Further we reported [25–30] that when two aromatic rings are separated by a group like  $-\text{SO}_2$ ,  $-\text{CH}_2$ ,  $-\text{C}=\text{O}$  and  $-\text{NH}$ , those molecules show TICT emission. Thus, it can be speculating than enhancement of LW emission should originate from the TICT state. The addition of CDs with aqueous solution of SMP and SMD the TICT band shows an enhancement with slight red shift, whereas the LE band shows a strong enhancement without changing its band position (Fig. 5).

The  $\beta$ -CD concentration dependent TICT emission intensities of SMP (Fig. 5) shows large enhancement when compared to aqueous  $\alpha$ -CD solution. In two ways the TICT emission could be possible when these drug molecules complex with  $\beta$ -CD. First the less polar medium of the inside cavity or the TICT state goes up causing an increase in the energy barrier for the transition from the LE to TICT state. So, in the event of non-radiative transition form LE gets trampled, the TICT emission enhanced. Secondly the SMP drug feels less geometrical restriction inside the  $\beta$ -CD cavity when compared to the  $\alpha$ -CD cavity. Hence, the free rotation of donor group was less hindered as this would cause further enhancement of the TICT emission. Earlier we have observed that TICT emission is strongly polarity sensitive [25–30] and very little enhancement TICT emission in  $\alpha$ -CD solutions suggest that this drug does not experience any major change in its polarity inside the  $\alpha$ -CD cavity when compared to that outside. From the above results it can be concluded that large enhancement of the TICT band of the SMP drug in

aqueous  $\beta$ -CD solution is due to less geometrical restriction and due to the larger size of the  $\beta$ -CD cavity ( $\sim 6.2 \text{ \AA}$ ) than that of  $\alpha$ -CD cavity ( $\sim 5.0 \text{ \AA}$ ). Benesi–Hildebrand plots pointed out that only a single type of 1:1 inclusion complexes are formed with the SMP with  $\alpha$ -CD and  $\beta$ -CD. Binding constant ( $K$ ) and free energy change values ( $\Delta G$ ) SMP/ $\alpha$ -CD and SMP/ $\beta$ -CD inclusion complexes are calculated by Benesi–Hildebrand equation. The calculated binding constant values for SMP/ $\alpha$ -CD complex are  $K_{\text{abs}} = 328 \text{ M}^{-1}$ ;  $K_{\text{flu}} = 735 \text{ M}^{-1}$  and SMP/ $\beta$ -CD complex are  $K_{\text{abs}} = 412 \text{ M}^{-1}$ ;  $K_{\text{flu}} = 783 \text{ M}^{-1}$ . The higher binding constant of SMP/ $\beta$ -CD inclusion complex suggests that SMP molecule form stable more inclusion complex with  $\beta$ -CD than compared with  $\alpha$ -CD. The experimental  $\Delta G$  values for SMP/ $\alpha$ -CD complex are given below:  $\Delta G_{\text{abs}} = -3.49 \text{ kcal mol}^{-1}$ ;  $\Delta G_{\text{flu}} = -3.97 \text{ kcal mol}^{-1}$  and SMP/ $\beta$ -CD complex are  $\Delta G_{\text{abs}} = -3.62 \text{ kcal mol}^{-1}$ ;  $\Delta G_{\text{flu}} = -4.01 \text{ kcal mol}^{-1}$ . The negative  $\Delta G$  of the inclusion complexes suggest that the inclusion preceded spontaneously at room temperature.

Fluorescence decay spectral analysis

The fluorescence decay behavior of aqueous SMP and its inclusion complexes were monitored by picosecond time correlated single photon counting spectrometer. Respective fluorescence decay profiles of aqueous SMP and corresponding complexes at pH  $\sim 7.0$  were monitored at 300 nm excited by SMP. Visual inspection of weighted residuals and reduced chi-square values indicate the necessity two exponentials to properly fit experimentally observed data points. Multi-exponential decays were significant for organic heterocyclics in solution and it is often difficult to mechanically assign the various components of decay. In the aqueous medium, four hydrogen bonding sites were present in the SMP molecule. The above behavior gives rise to different charge distribution structures with varying fluorescence decay life times. As an alternative of giving importance to individual decay components, we defined the second order average life time ( $\tau$ ) SMP in solution using as described in Paul and Guchhat [31]. The SMP drug in water shows an average lifetime of 0.77 ns, which comparatively is very lower than that of SMP/ $\alpha$ -CD (2.54 ns) and SMP/ $\beta$ -CD (1.65 ns). These results indicated that the nonradiative transition of SMP drug was affected in the corresponding CD solution, which is in turn responsible for the increase in the lifetime of the CD solution. The overall result suggests that SMP complexes with  $\alpha$ -CD and  $\beta$ -CD form stable system.

Semiempirical quantum mechanical calculations

In order to support the inclusion process, we applied semiempirical quantum mechanical calculations at PM3 level of theory. Binding energies, complexation enthalpy, entropy, free energy changes and HOMO–LUMO energy levels of the SMP drug and its inclusion complexes are listed in Table 1. The data presented in Table 1 clearly indicates that these SMP/CD inclusion complexes were formed because of their negative binding energies and that the bigger absolute negative values led to the higher stability of these complexes. Fan and his co-workers [32] proved that the higher negative binding energy values of complexes have higher stability than others. The complexation energies of SMP/ $\alpha$ -CD =  $-19.63 \text{ kcal mol}^{-1}$  and SMP/ $\beta$ -CD =  $-22.50 \text{ kcal mol}^{-1}$ . Among the two complexes SMP/ $\beta$ -CD complex was more stable than SMP/ $\alpha$ -CD. This higher stability of the complexes was dependent upon the number of hydrogen bonds formed between the host and guest molecules. Since the SMP/ $\beta$ -CD complex have two hydrogen bonds (Fig. 6), it is more stable than SMP/ $\alpha$ -CD. Morokuma [33] have demonstrated that the hydrogen bonding effects the formation of the energy of the complexes and also their report revealed that the PM3 level of semiempirical calculations is more suitable for the study of these types of inclusion complex process. Further, the complexation energy of SMP/CD inclusion complexes is higher negative values than the corresponding free SMP molecule which suggests that the formed complexes are more stable than the corresponding free molecules. In addition to the hydrogen bonds, the hydrophobic interaction also contributed in a major way toward the stabilities of the complexes. The hydrophobic CD cavities behaved as a binding acceptor to aromatic rings like benzene and naphthalene moiety of guests which is also one of the factors that stabilized the inclusion complexes.

The HOMO energies, LUMO energies and HOMO–LUMO energy gap of free SMP and its inclusion complexes were listed in Table 1. The HOMO, LUMO energy orbital pictures of the SMP molecule is shown in Fig. 7. The HOMO and LUMO energy gap of the SMP/ $\alpha$ -CD inclusion complex was more negative ( $-8.1 \text{ eV}$ ) than SMP/ $\beta$ -CD. Therefore, SMP/ $\alpha$ -CD complex is more stable than others. The above higher energy gap was due to the hydrogen bonding interaction between the host and guest. This interaction changed the electronic structure of the complexes to a certain extent, leading to the elevation of HOMO energy and the depression of LUMO energy in the SMP/ $\alpha$ -CD complex. The net Mulliken charges of these four

Table 1 Energetic features, thermodynamic parameters and HOMO–LUMO energy calculations for SMP, SMD and its inclusion complexes by PM3 method.

Properties	SMP	$\alpha$ -CD	$\beta$ -CD	SMP/ $\alpha$ -CD	SMP/ $\beta$ -CD
$E_{\text{HOMO}}$ (eV)	-9.03	-10.37	-10.35	-9.35	-9.01
$E_{\text{LUMO}}$ (eV)	-0.68	1.26	1.23	-1.17	-0.92
$E_{\text{HOMO}}-E_{\text{LUMO}}$ (eV)	-8.35	-11.63	-11.58	-8.18	-8.09
$\mu$	-4.85	-4.56	-4.56	-5.26	-4.96
$\eta$	4.17	5.81	5.79	4.10	4.04
$\omega$	2.82	1.78	1.79	3.13	3.05
$S$	0.23	0.17	0.17	0.24	0.25
Dipole ( $D$ )	5.64	11.34	12.29	6.81	5.94
$E^a$	-26.06	-1247.62	-1457.63	-1254.05	-1506.19
$\Delta E^a$				-19.63	-22.50
$G^a$	86.47	-676.37	-789.52	-533.57	-701.13
$\Delta G^a$				56.32	1.92
$H^a$	128.91	-570.84	-667.55	-405.33	-558.91
$\Delta H^a$				36.60	-7.54
$S^b$	0.142	0.353	0.409	0.430	0.476
$\Delta S^b$				-0.065	-0.075
Zero point vibrational energy <sup>a</sup>	142.99	635.09	740.56	795.54	887.33
Mulliken properties	0.00	0.00	0.00	0.00	0.00

<sup>a</sup> kcal mole<sup>-1</sup>.  
<sup>b</sup> kcal/mol K.

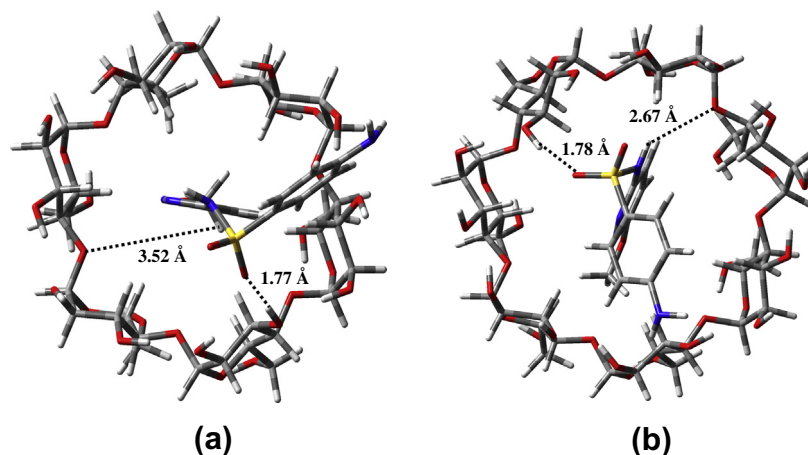


**Fig. 6.** PM3 optimized structure of (a) SMP/ $\alpha$ -CD and (b) SMP/ $\beta$ -CD inclusion complexes; Colors of the atoms denotes: Blue ~ nitrogen, yellow ~ sulphur, red ~ oxygen, white ~ hydrogen, and grey ~ carbon of the molecules respectively. (For interpretation of the references to colour in this figure legend, the reader is referred to the web version of this article.)

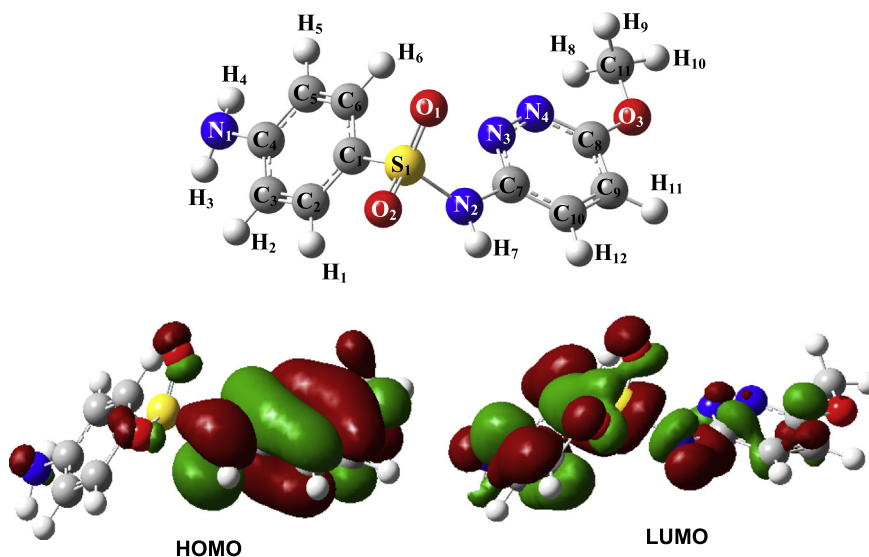


**Fig. 7.** Optimized structure and HOMO–LUMO energy structures of SMP; Colors of the atoms denotes Blue ~ nitrogen, yellow ~ sulphur, pale red ~ oxygen, white ~ hydrogen, grey ~ carbon and whereas the green and dark red colors indicate negative and positive phase of the molecules respectively. (For interpretation of the references to colour in this figure legend, the reader is referred to the web version of this article.)

complexes were zero and this result indicates that there is no charge transfer interaction present in these complexes. The CD cavities could offer a nonpolar environment but also attract the electrons if the guests were matched with host (CD) both in space and in electric charges which pronounces the binding process. Further the dipole moments of both the inclusion complexes were lying between the dipole moments of the free guest and host. For example, the dipole moment value of SMP/ $\alpha$ -CD complex is 6.81 D, lies between the values of free SMP (5.64 D) and  $\alpha$ -CD (11.34 D). The above result is due to the guest molecule where transferred polar environment to less polar or even nonpolar CD cavities.

Chemical potential ( $\mu$ ), stability ( $S$ ), hardness ( $\eta$ ) and electrophilicity ( $\omega$ ) of the isolated SMP and its inclusion complexes were listed in Table 1. From Table 1 following points can be observed (i) SMP/ $\alpha$ -CD complex having higher negative chemical potential than others, (ii) hardness of the SMP molecule is decreased in the SMP/ $\alpha$ -CD and SMP/ $\beta$ -CD inclusion complexes, (iii) whereas the electrophilicity of the SMP molecule is increased in the SMP/ $\alpha$ -CD

and SMP/ $\beta$ -CD inclusion complexes and (iv) no significant difference in the stability of the SMP/CD complexes.

The global minimum energy geometries were used to estimate the thermodynamic quantities ( $\Delta G$ ,  $\Delta H$  and  $\Delta S$ ) of the inclusion process of SMP/CD inclusion complexes. The thermodynamic quantities of both the inclusion complexes are listed in Table 1. The lower level of the computational calculation method was not able to reproduce absolute free energy changes of the complexation process were due to the limitations of the semiempirical calculations at PM3 level. Quantitatively, the miscalculation seems to be addressed to a systematic over estimation of the free energy changes ( $\Delta G$ ) of the inclusion complexes as displayed in Table 1. From Table 1, it can be observed that the complex process have positive free energy change values which suggests that these inclusion processes are not spontaneous processes. But generally the inclusion processes are spontaneous occurrence at room temperature. The above contradict results are arise not only due to the limitations of PM3 level calculations but also due to optimization of

**Table 2**  
Geometrical parameters of SMP before and after inclusion with  $\alpha$ -CD and  $\beta$ -CD for the most stable inclusion complexes.

	SMP	SMP/ $\alpha$ -CD	SMP/ $\beta$ -CD
<i>Bond length (Å)</i>			
H <sub>4</sub> –H <sub>9</sub>	10.26	11.05	11.53
H <sub>3</sub> –H <sub>9</sub>	9.41	9.86	10.02
H <sub>6</sub> –H <sub>1</sub>	4.36	4.33	4.32
H <sub>4</sub> –C <sub>11</sub>	9.31	10.54	9.06
H <sub>11</sub> –N <sub>4</sub>	3.48	3.43	3.42
<i>H-bond length (Å)</i>			
(–NH)H–O (glycoside)	3.52	2.67	
(–SO <sub>2</sub> )O–H(2 <sup>o</sup> OH)	1.77	1.78	
<i>Bond angle (°)</i>			
H <sub>4</sub> –N <sub>1</sub> –C <sub>4</sub>	112.74	113.63	113.24
C <sub>1</sub> –S <sub>1</sub> –O <sub>1</sub>	112.38	111.35	112.99
S <sub>1</sub> –N <sub>2</sub> –C <sub>7</sub>	128.93	124.59	127.23
C <sub>8</sub> –O <sub>3</sub> –C <sub>11</sub>	101.67	116.90	118.06
<i>Dihedral angle (°)</i>			
C <sub>1</sub> –S <sub>1</sub> –N <sub>1</sub> –C <sub>7</sub>	78.41	107.62	72.69
C <sub>1</sub> –S <sub>1</sub> –N <sub>1</sub> –H <sub>7</sub>	–128.09	–109.38	–137.26
H <sub>4</sub> –N <sub>1</sub> –C <sub>4</sub> –C <sub>5</sub>	27.94	24.03	28.52

inclusion complexes in a vacuum. Since, we neglect the solvent parameters in the thermodynamic calculations that become the factors for the above controversial results.

The negative enthalpy changes ( $\Delta H$ ) of the SMP/ $\beta$ -CD ( $-7.54 \text{ kcal mol}^{-1}$ ) complex reveals that this complexation process is an enthalpy driven process. Similarly the negative entropy changes ( $\Delta S$ ) were observed in the thermodynamic calculations, where the quantity of the entropy changes is very minimal for both inclusion complexation processes. The SMP/ $\beta$ -CD complex shows a high entropy change ( $-0.075 \text{ kcal mol}^{-1}$ ) than SMP/ $\alpha$ -CD complex. The above result suggests that the inclusion processes are not only enthalpy driven but also entropy co-driven processes.

Table 2 depicts the selected geometrical parameters like bond distance, bond angles, dihedral angles and hydrogen bonding distances of SMP before and after inclusion with CDs. From Table 2 it can be seen that only minimum changes are formed in the bond distance and bond angles, but a significant change can be observed in the dihedral angles. For example, the vertical distance of the SMP molecule is 10.26 Å but it changes 11.64 Å in the  $\alpha$ -CD complexes. Likewise, the dihedral angle of bonds between C<sub>1</sub>–S<sub>1</sub>–N<sub>1</sub>–C<sub>7</sub> in free SMP is  $-29.4^\circ$ , but this is considerably changed to  $-54.6^\circ$  in  $\alpha$ -CD complexes. The overall annotation from the geometrical parameters (Table 2) suggests that the SMP molecules adopt a specific conformation in the CDs cavities.

## Conclusions

In summary, we have fabricated that a supramolecular 2D nanosheet aggregate in aqueous solution composed of SMP and  $\beta$ -CD. The inclusion complexes of SMP/ $\beta$ -CD first formed a pseudopolyrotaxane like structure through hydrogen bonding interactions and then these pseudopolyrotaxanes were primary assembled to form 1D molecular level nanosheet. Further, these 1D molecular level nanosheets are secondary self assembled to form 2D nanosheet through staking interaction between the sheets. But in the case of SMP/ $\alpha$ -CD inclusion complexes form the nanorods through self assembly process. The intermolecular hydrogen bonding and van der Waals forces are the main dominant driving force for the construction of this type of supramolecular architecture. The reasonable self assembling mechanism of the formation of this 2D nanosheet is suggested based on the results

observed from SEM, TEM and molecular modeling calculations. In order to confirm the interactions between SMP and CDs a detailed characterization was carried out by using FT-IR, P-XRD, DSC, <sup>1</sup>H NMR, absorption spectroscopy, fluorescence emission spectroscopy and lifetime measurements.

## Acknowledgements

This work was supported by the Council of Scientific and Industrial Research [No. 01(2549)/12/ EMR-II] and the University Grants Commission [F.No. 41-351/2012 (SR)] New Delhi, India. One of the authors, G. Venkatesh is thankful to the University Grants Commission, New Delhi, India for the award of BSR-SAP fellowship. The authors thank Dr. P. Ramamurthy, Director, National Centre for ultrafast processes, Madras University for allowing the fluorescence lifetime measurements for this work.

## Appendix A. Supplementary material

Supplementary data associated with this article can be found, in the online version, at <http://dx.doi.org/10.1016/j.saa.2013.12.053>.

## References

- R. Auzely-Velty, S. Djedaini-Pilard, S. Desert, B. Perly, T.H. Zemb, *Langmuir* 16 (2000) 3727–3734.
- B.J. Ravoo, R. Darcy, P. Gambadauro, F. Mallamace, *Langmuir* 18 (2002) 1945–1948.
- R. Donohue, A. Mazzaglia, B.J. Ravoo, R. Darcy, *Chem. Commun.* (2002) 2864–2865.
- B.J. Ravoo, R. Darcy, *Angew. Chem.* 112 (2000) 4494–4496.
- D. Duchene, G. Ponchel, D. Wouessidjewe, *Adv. Drug Deliv. Rev.* 36 (1999) 29–40.
- E. Memisoglu, A. Bochot, M. Sen, D. Charon, D. Duchene, A.A. Hincal, *J. Pharm. Sci.* 91 (2002) 1214–1224.
- A. Geze, S. Aous, I. Baussanne, J.L. Putaux, J. Defaye, D. Wouessidjewe, *Int. J. Pharm.* 242 (2002) 301–305.
- V.K. Lamer, R.H. Dinegar, *J. Am. Chem. Soc.* 72 (1950) 4847–4854.
- H. Fessi, F. Puisieux, J.P. Devissaguet, N. Ammoury, S. Benita, *Int. J. Pharm.* 55 (1989) R1–R4.
- A. Geze, J.L. Putaux, L. Choïnard, P. Jehan, D. Wouessidjewe, *J. Microencapsulation* 21 (2004) 607–613.
- M.V. Rekharsky, Y. Inoue, *Chem. Rev.* 98 (1998) 1875–1918.
- R. Villalonga, R. Cao, A. Frago, *Chem. Rev.* 107 (2007) 3088–3116.
- K. Ukeama, F. Hirayama, T. Irie, *Chem. Rev.* 98 (1998) 2045–2076.
- Y. Xia, K.E. Rodgers, J. Paul, G.M. Whitesides, *Chem. Rev.* 99 (1999) 1823–1848.
- S.J. Hashimoto, J.K. Thomas, *Am. Chem. Soc.* 107 (1985) 4655–4662.
- J. Premakumari, G. Allan Gnana Roy, A. Antony Muthu Prabhu, G. Venkatesh, V.K. Subramanian, N. Rajendiran, *Phys. Chem. Liq.* 49 (2011) 108–132.
- A. Antony Muthu Prabhu, G. Venkatesh, N. Rajendiran, *J. Soln. Chem.* 39 (2010) 1061–1086.
- T. Steiner, G.J. Koellner, *Am. Chem. Soc.* 116 (1994) 5122–5128.
- A.A. Rafati, S.M. Hashemianzadeh, Z.B. Nojini, M.A. Safarpour, *J. Mol. Liq.* 135 (2007) 153–157.
- P. Das, A. Mallick, D. Sarkar, N. Chattopadhyay, *J. Phys. Chem. C* 112 (2008) 9600–9603.
- J.H. Park, S. Hwang, J. Kwak, *ACS Nano* 4 (2010) 3949–3958.
- N. Chandrasekhar, R. Chandrasekar, *Angew. Chem. Int. Ed.* 51 (2012) 3556–3561.
- D. Chen, Q. Lu, X. Jiao, *Chem. Mater.* 17 (2005) 4168–4173.
- T.L. Neoh, H. Yoshi, T.J. Furta, *J. Incl. Phenom. Macrocycl. Chem.* 56 (2006) 125–133.
- A.A. Smith, K. Kannan, R. Manavalan, N. Rajendiran, *J. Fluorescence* 20 (2010) 809–820.
- K. Sivakumar, T. Stalin, N. Rajendiran, *Spectrochim. Acta* 62A (2005) 991–999.
- A. Antony Muthu Prabhu, R.K. Sankaranarayanan, G. Venkatesh, N. Rajendiran, A. Antony, *J. Phys. Chem. B* 166 (2012) 9061–9074.
- A. Antony Muthu Prabhu, R.K. Sankaranarayanan, S.SivaN. Rajendiran, *Spectrochim. Acta A* 74 (2009) 484–497.
- A. Anton Smith, K. Kannan, R. Manavalan, N. Rajendiran, *J. Inclusion Phenom. Macrocycl. Chem.* 58 (2007) 161–167.
- A.A.M. Prabhu, N. Rajendiran, *J. Fluorescence* 22 (2012) 1461–1474.
- B. Kumar Paul, N. Guchhait, *J. Colloid Interface Sci.* 353 (2011) 237–247.
- X.X. Fan, Y. Yang, S. Shung, C. Dong, *Spectrochim. Acta A* 61 (2005) 953–959.
- K. Morokuma, *Acc. Chem. Res.* 10 (1977) 294–300.